Arabian Journal for Science and Engineering (2020) 45:729–741
https://doi.org/10.1007/s13369-019-04133-w

RESEARCH ARTICLE - MECHANICAL ENGINEERING

Parametric Study and Comparison of Aerodynamics Momentum-Based Models for Straight-Bladed Vertical Axis Wind Turbines

Amin A. Mohammed[1] · Hassen M. Ouakad[2] · Ahmet Z. Sahin[1] · Haitham M. S. Bahaidarah[1]

Received: 4 April 2019 / Accepted: 11 September 2019 / Published online: 23 September 2019
© King Fahd University of Petroleum & Minerals 2019

Abstract
In this study, different momentum models for vertical axis wind turbines (VAWTs) are investigated and compared for different operating parameters. The performance over different rotor solidities and aspect ratios is studied to find the best configuration of the turbine. By comparing different models, the merit of double multiple streamtube model is established. Three different airfoils were investigated using the parameters of reference turbines from the literature. NACA0015 is found to be advantageous among NACA0012 and NACA0021. Also, the effect of different number of blades is studied and it is found that two-bladed rotor with NACA0015 airfoil provides excellent performance. By studying the turbine aspect ratio, it is found that a VAWT of 5.1 m height and 4.25 m diameter will generate a maximum power coefficient of 36.13% at TSR of 5.51 with good starting behavior.

Keywords Momentum models · VAWT · Aerodynamics · Streamtube · DMST model

List of Symbols

C_P	Power coefficient
P	Power (W)
Q, T	Aerodynamic torque (N m)
N	Number of blades
c	Chord length of the blade (m)
R, D	Radius/diameter of the wind turbine (m)
H	Height of the blade/turbine (m)
σ	Solidity ($\sigma = Nc/R$)
λ	Tip-speed ratio (TSR), $\lambda = \frac{\omega R}{V_\infty}$
ω	Rotor angular velocity (rad/s)
V_a	Upstream induced velocity (m/s)
V_∞	Free stream velocity (m/s)
V_a^d	Downstream induced velocity (m/s)
W	Relative velocity upstream (m/s)
W^d	Relative velocity downstream (m/s)
V_c	Chordal velocity component (m/s)
V_n	Normal velocity component (m/s)
θ	Azimuth angle
α	Angle of attach
α_d	Downstream angle of attach
q	Local relative dynamic pressure (N/m^2)
$\Delta\theta$	Azimuth angle increment correspond to one streamtube
N_θ	Number of θ increments $\left(N_\theta = \frac{\pi}{\Delta\theta} + 1\right)$
T_B	Torque on a complete blade (N m)
C_l	Airfoil lift coefficient
C_d	Airfoil drag coefficient
C_t	Tangential coefficient
C_n	Normal coefficient
ρ	Density of the air (kg/m^3)
F_D	Streamwise drag force (N)
C_{DD}	Rotor drag coefficient
C_D	Drag coefficient
A	Rotor/turbine swept area, (m^2) ($A = 2HR$)
a, a^d	Upwind and downwind induction factors
f_u, f_d	Upwind and downwind functions
F_t, F_n	Normal and tangential force (N)
F_{ta}	Average tangential force (N)
F_x	Streamwise force (N)
$\bar{F}_x$	Average streamwise force (N)
F_x^*	Non-dimensional streamwise force

Abbreviations

VAWT	Vertical axis wind turbine
SB-VAWT	Straight-bladed vertical axis wind turbine
HAWT	Horizontal-axis wind turbine
SST	Single streamtube

✉ Hassen M. Ouakad
houakad@squ.edu.om

[1] Mechanical Engineering Department, King Fahd University of Petroleum and Minerals, Dhahran 31261, Saudi Arabia

[2] Department of Mechanical and Industrial Engineering, Sultan Qaboos University, Al-Khoud, 123 Muscat, Oman

MST Multiple streamtube
DMST Double multiple streamtube
RMSE Root-mean-squared error

1 Introduction

With the continuous increase in the oil/gas and fossil fuels prices coupled with their environmental pitfalls, many researchers got motivated to investigate renewable energy harvesting such as wind-based energy harvesters [1, 2]. In Saudi Arabia, several studies have focused on renewable/wind energy characterization and investigation [3–5]. To extract energy from the wind, different technologies were assumed [6]. VAWTs play significant role in this regard. The evolution of the principal VAWT's types containing Savonius, Giromill and Darrieus designs were summarized in [7]. To demonstrate how to analyze the intricate aerodynamics of such machines utilizing a reasonably straightforward approach, an overview of the DMST model for VAWT was introduced. The study also highlighted that the Darrieus turbine is the best suited VAWT for implementation of electricity production to utility scale. As displayed in Fig. 1, the most popular types of VAWTs are Savonius and Darrieus turbine (curved and straight bladed) [8]. Jin. et al. [9] reviewed the fundamental research methods for Darrieus VAWTs.

The performance of VAWTs is affected by several parameters including wind speed, blade size, airfoil type, turbine aspect ratio, tip-speed ratio (TSR) and rotor solidity. These parameters and others make it very complicated to effectively identify which parameter should be changed to improve the power coefficient of the turbine which justify the necessity for parametric study. In [10] the effect of the turbine aspect ratio (H/R) on turbine power coefficient is presented. It was reported that lower aspect ratio provides higher performance and better structural properties of the rotor. Moreover, the effect of solidity on the aerodynamic performance of urban VAWTs has been investigated in [11]. The obtained results showed that, "(i) low solidity is favorable for fixed-rotational-speed urban VAWTs due to their inevitable high tip-speed ratio, (ii) solidity of fixed-rotational-speed VAWTs needs to be selected with special attention to the wind conditions of potential installation sites and (iii) the optimal design for VAWTs needs to include variable rotational speed, high solidity and low tip-speed ratio".

In another study by Kanyako et al. [12] the effect of different parameters such as blade profile and number of the blades on the performance of a VAWT was investigated in a low- and high-fidelity analysis using a DMST model and CFD simulations. The DMST model and numerical analysis of VAWT is proposed in [13], in which NACA0018 was selected for a fixed pitch turbine. Negative torque was observed at lower TSR using the DMST model, yet the results obtained numerically by CFD had proven that the turbine could generate positive torque at lower TSR.

VAWTs play significant role in remote locations away from the main grid where small-scale VAWT and rooftop designs are utilized to supply electricity for buildings. Aerodynamic properties of building integrated VAWT have been studied in [14], where numerical and experimental investigations have been carried out. The obtained results showed that the aerodynamic performance of such turbine is sensitive to the wind direction. Moreover, different solidities, airfoils and architectural configurations were found to have a great influence on the aerodynamic performance. Normally, VAWTs with larger solidity and thicker blades have priority to choose. Comparatively, thick airfoils are suggested for VAWTs to lessen fatigue loading on blades [15].

An economical evaluation and aerodynamic design of site-specific small VAWTs were explored in [16]. The DMST model and BEM theory were used in the design

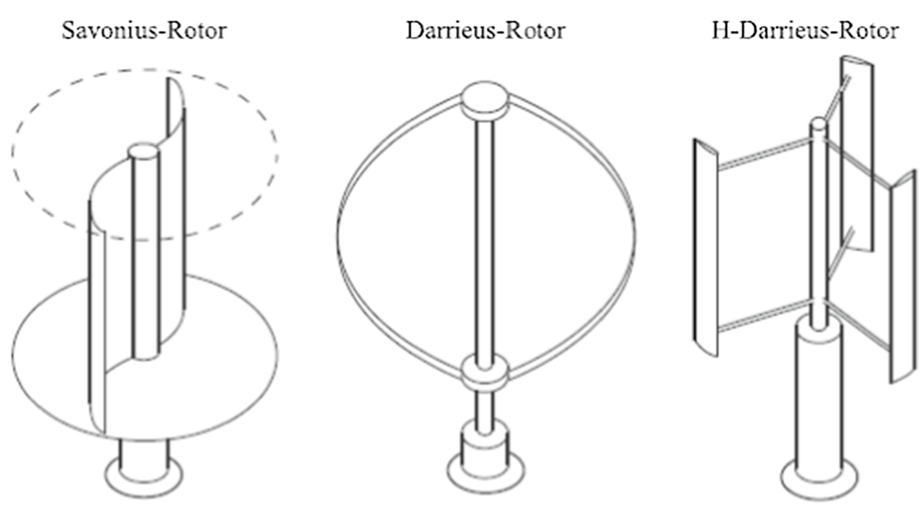

Fig. 1 Types of vertical axis wind turbines [8]

and optimization of the site-specific H-rotor. A parametric study was performed, and the obtained results showed almost a 50% saving in the cost of the electricity generated by the site-specific H-rotor VAWT. Moreover, in [17] numerical investigation of a vertical axis tidal turbine having a deformable blades is proposed. The leading edge of the blade has been deformed using a sinusoidal smoothed curve. Testing the shed vortices interactions and the associated contours of the pressure showed that the modification of the leading edge led rise to a vortex with large size at a promoted stage than the traditional blade. The efficiency was improved by 35% compared to the uncontrolled instance.

For performance improvement and accurately predicting the structural behavior of VAWTs, their interaction with the wind must be studied which is the subject of the aerodynamic modeling. Among different models, streamtube models (momentum models) are widely used. Moreover, blade pitching could readily be incorporated to further enhance the starting torque capacity and performance of such designs. In this study, different momentum models are investigated and compared for different operating parameters. The main objective of this paper is to compare the performance of SB-VAWT utilizing momentum models under different airfoils, number of blades, solidity and aspect ratio. We selected momentum models because they are very popular and relatively straightforward to implement [18, p. 2]. Therefore, streamtube models might be used by researchers and engineers to predict the turbine performance in the design stage. Moreover, the effect of rotor solidity will be investigated by changing both the chord of the blade and then by changing the number of blades. Finally, the effect of turbine aspect ratio will be studied to find the best configuration that will provide reasonable performance.

2 Momentum Models

Momentum models are essentially based on the calculation of flow velocity across the turbine by equating the streamwise aerodynamic force on the blades, which is equal to the average pressure difference across the rotor, with the rate of change of momentum of the air (mass flow rate times the overall velocity change). Afterward, Bernoulli's equation is applied in each streamtube. The major obstacle of these models is that they become invalid for large tip-speed ratios and for high rotor solidities because the momentum equations in such cases are inadequate [19]. There are three types of momentum models which will be detailed in subsequent headings.

2.1 Single Streamtube (SST) Model

In 1974, Templin proposed the SST model which is the first and most simple prediction method for calculating the performance characteristics of Darrieus-type VAWTs [20]. A representation of SST is sketched in Fig. 2 where a constant induced velocity is assumed.

According to SST model, the power coefficient (C_P) is given by Eq. 1, more details are given in "Appendix A."

$$C_P = \frac{P}{P_{max}} = \frac{27}{32}\frac{1}{2\pi}\frac{Nc}{R}\frac{R\omega}{V_a}\left(\frac{V_a}{V_\infty}\right)^3 \int_0^{2\pi}\left(\frac{q}{\frac{1}{2}\rho V_a^2}\right)C_t d\theta \quad (1)$$

2.2 Multiple Streamtube (MST) Model

To overcome the limitations of SST model (fixed induced velocity), a MST model for Darrieus-type VAWT is introduced by Strickland [21]. In this model, momentum variations and blade elemental forces along each streamtube are equated to obtain the induced velocity. The MST model is constructed by dividing the turbine's swept volume into a series of adjacent, aerodynamically independent parallel streamtubes as given in Fig. 3. This model was also studied by Sanyer et al. [22] in his master thesis.

The power coefficient is given as follows (more details are given in "Appendix A"):

$$C_P = \frac{\sum_1^{N_\theta} \frac{Nc}{2R}\lambda\left(\frac{W}{V_\infty}\right)^2 C_t}{N_\theta} \quad (2)$$

where λ is the TSR, N_θ number of θ increments and W is the relative velocity.

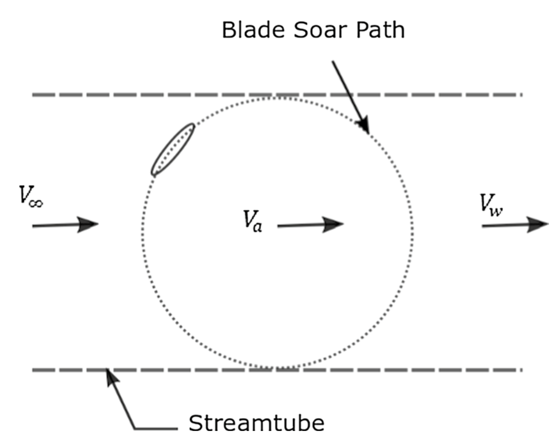

Fig. 2 Schematic diagram of single streamtube model

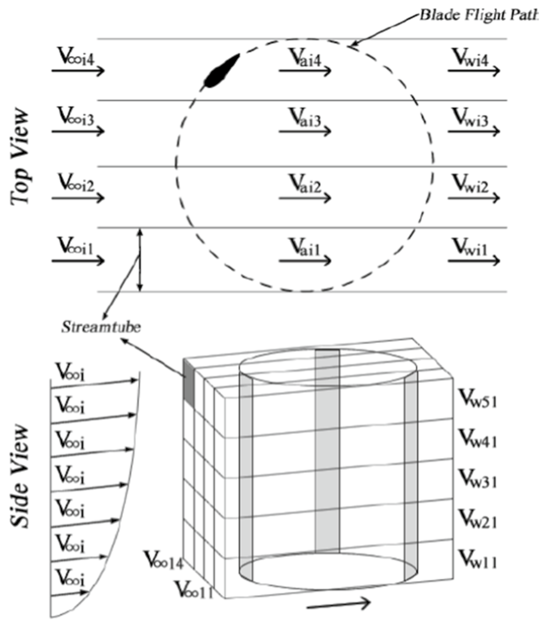

Fig. 3 Diagrammatic sketch of multiple streamtube model [23]

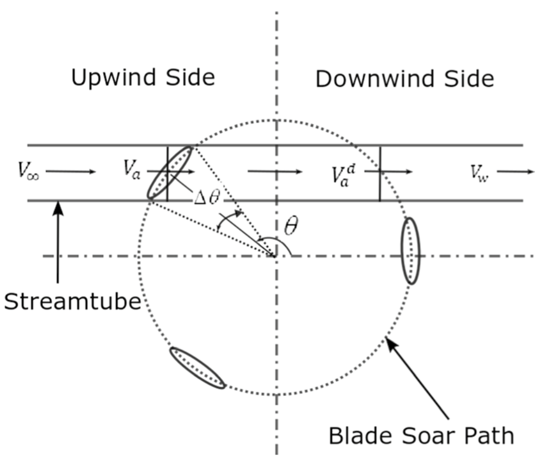

Fig. 4 Diagram describing the DMST model

2.3 DMST Model

The DMST proposed by Paraschivoiu [24] joins the MST model with the double actuator disk theory to determine the performance of Darrieus wind turbine. In DMST model, the calculation is carried out separately for the upwind and downwind parts of the turbine as presented in Fig. 4.

This model solves two equations concurrently for the streamwise force at the actuator disk; one is built on the aerodynamic coefficients and the local wind speed and the other found by momentum conservation. These equations are solved twice: for the upstream and downstream half cycles. The power coefficient for the upwind half of the turbine is given by:

$$C_{P_u} = \frac{NcH}{2\pi A} \int_{\pi/2}^{3\pi/2} C_t \left(\frac{W}{V_\infty} \right)^2 d\theta \qquad (3)$$

where H is the length of the blade (height of the turbine) and A is the rotor/turbine swept area.

The downwind part of the rotor is treated in the same manner and to find the overall power coefficient of the rotor, the power coefficients of the two half cycles are eventually summed. The blade profiles considered in this study along with a two-bladed rotor [25] are sketched in Fig. 5.

3 Validation of the Models

Momentum models have been popularly used for aerodynamic performance of VAWTs, especially the DMST model, and the results have confirmed that the models can provide reasonable accuracy [26, 27]. For numerical calculations, all the models are programmed in MATLAB. In this document, the model validation was utilized to establish the correction of the programing process rather than to test the accuracy of the mathematical models.

3.1 SST Model

Comprehensive experimental results in the literature are available for the curved blade (Φ-type) VAWTs; however, limited results have been reported about H-rotors. Thus, for performance evaluation and testing using SST model, we considered a two-bladed-curved blade Darrieus turbine tested at the Sandia National Laboratories for comparison [21]. The turbine parameters are: $H = 2$ m, $D = 2$ m and $c = 0.09$ m and utilized the NACA0012 airfoil. The data for lift and drag are taken from a key publication by Sheldahl et al. [28]. The obtained results are given in Fig. 6 where considerable match between the results is achieved.

Moreover, the performance was investigated over a range of solidities ($\sigma = \frac{Nc}{R}$) using SST model as shown in Fig. 7. Turbine power coefficient gets improved by increasing the rotor solidity, nevertheless for a limited TSR range and with poorer starting capacity.

3.2 MST Model

For a two-bladed (H-rotor) VAWT having a radius of 0.904 m, aspect ratio (H/R) of 2, free stream velocity of 10 m/s considering NACA0018 airfoil at 5×10^6 Reynolds number investigated by Brusca et al. [10], the following results are obtained as supplied in Fig. 8.

With a chord of 0.0904 m the solidity is 0.2. The airfoil characteristics for lift and drag coefficients are taken

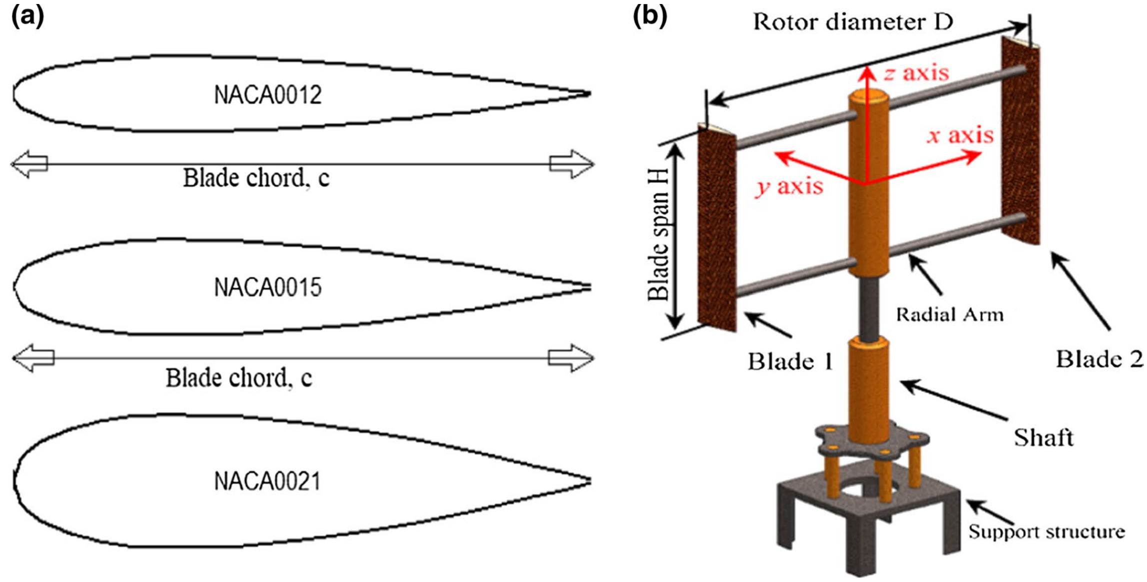

Fig. 5 **a** Sketch of the three NACA airfoils used and **b** SB-VAWT of two blades [25]

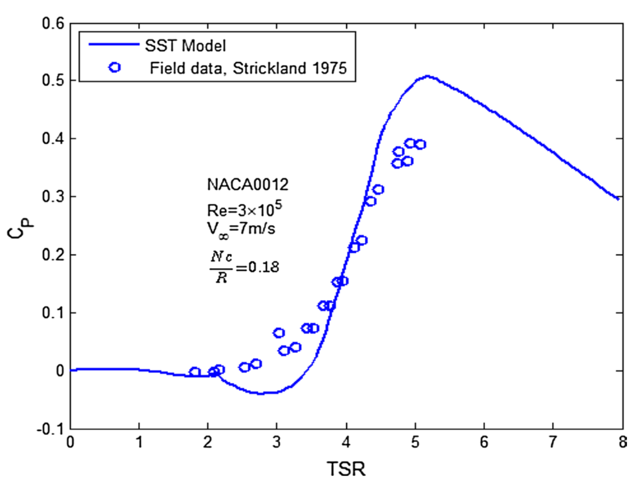

Fig. 6 Power coefficient for a SB-VAWT using SST model

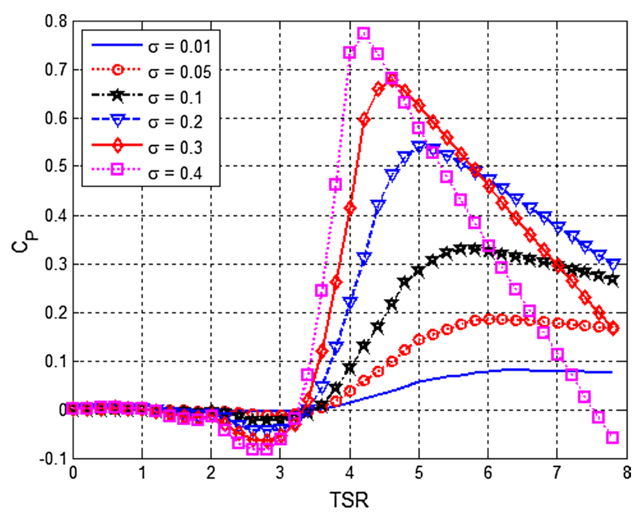

Fig. 7 Power coefficient for a SB-VAWT using SST model over a range of solidities

from the previous Ref. [28]. It is obvious that the current model is in fairly agreement with previous work. Though Brusca's results show a higher power coefficient for a TSR between 3 and 6, it is advantageous for the current results as MST model seems to overpredict the power coefficient in many cases; this will be clear when the current results are compared with experimental data in Sect. 4. Figure 9 presents the performance of MST model over a range of solidities. As shown, for low solidity we obtain a fair power coefficient for a wide range of TSR. However, for higher solidities though the performance is improved, yet, for a limited TSR. Thus, the process must be optimized to get a good power coefficient.

3.3 DMST Model

Considering the same reference turbine used in Sect. 3.1, a DMST model is implemented. The obtained results are given in Fig. 10. As shown, there is some discrepancy among the results, and this is perhaps because the field data are for a CB-VAWT, whereas a SB-VAWT is being investigated in this study.

To evaluate the effectiveness of DMST model further, a 5-m-diameter Darrieus turbine tested at Sandia wind turbine laboratories [29], having the properties in Table 1 (approximated), was used to compare the modeling results

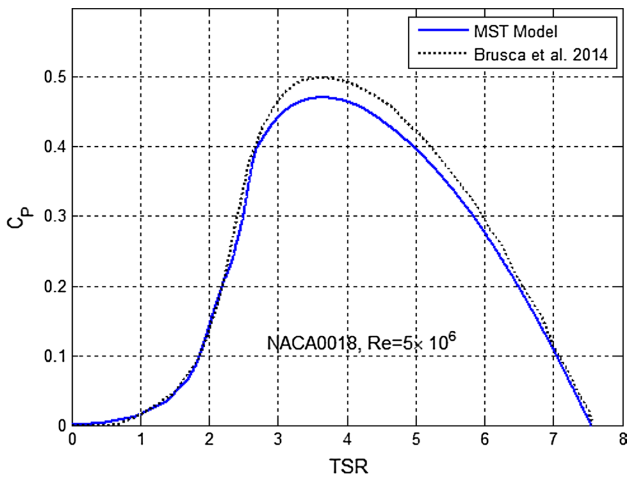

Fig. 8 Power coefficient for a SB-VAWT using MST model

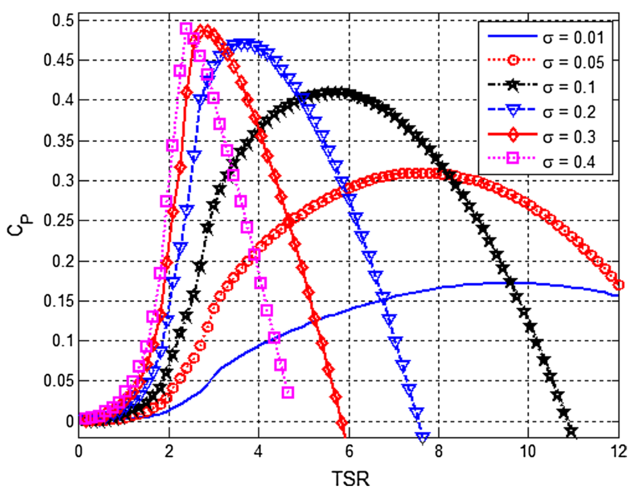

Fig. 9 Power coefficient for a SB-VAWT using MST model over a range of solidities

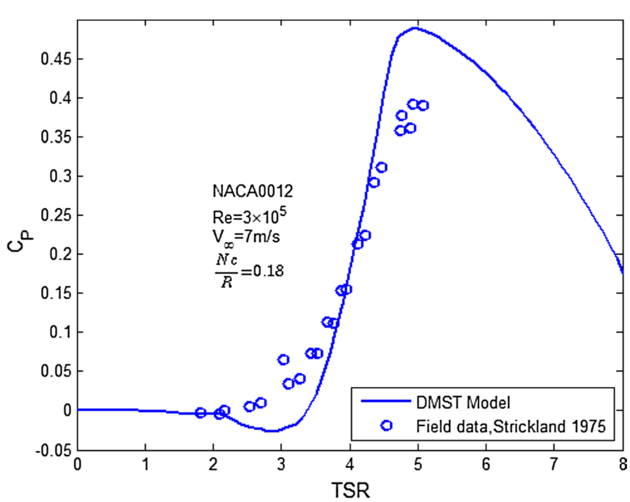

Fig. 10 Comparison of DMST with experimental data

Table 1 Properties of 5 m Darrieus turbine [29]

Number of blades	2
Radius (m)	2.5
Chord (m)	0.1524
Blade length (m)	5.1
Airfoils	NACA0015
Re	330,000
Rotational speed (rpm)	162.5

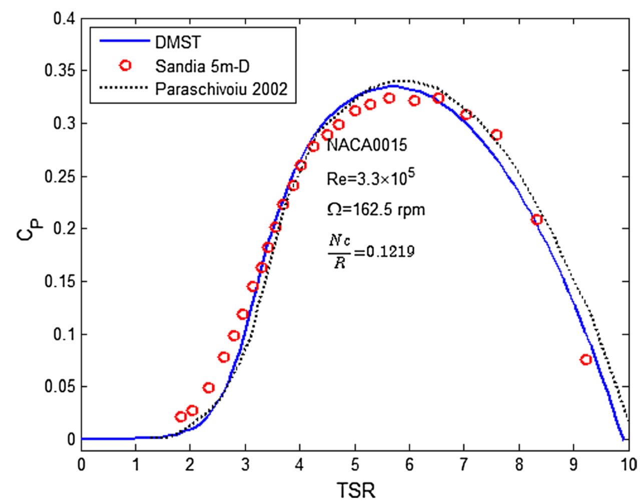

Fig. 11 Comparison of DMST model with experimental and other results

with the experimental data. The obtained results were further compared with Paraschivoiu [19]. The achieved results are displayed in Fig. 11 where excellent agreement among the results is obtained which confirms the correctness of DMST implementation.

In Fig. 12, the performance over a range of solidites is presented. As displayed, the turbine almost generated no power for a solidity as low as 0.01. However, the power coefficient gradually increases by increasing the rotor solidity up to 0.16, beyond which the solution is not converging.

4 Results and Discussion

This section presents the obtained results using different models for comparison purposes. Moreover, a parametric study using different number of blades (different solidities), different airfoils and various aspect ratios is also proposed.

4.1 Comparison of the Models

Considering the 2 m wind turbine mentioned earlier [21], the results of SST, MST and DMST models are compared

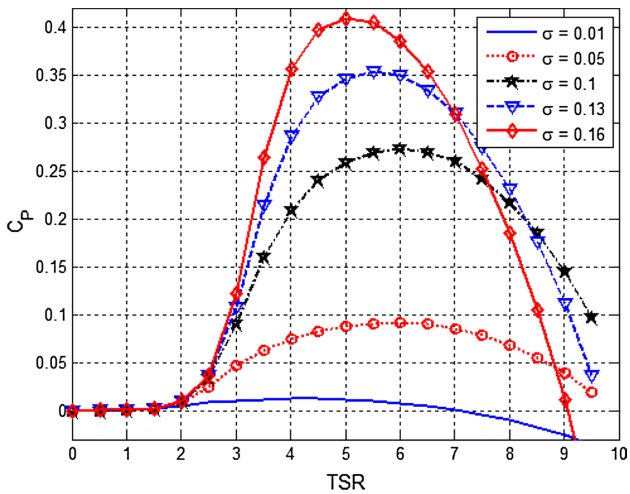

Fig. 12 Power coefficient for Sandia 5 m rotor using DMST model over a range of solidities

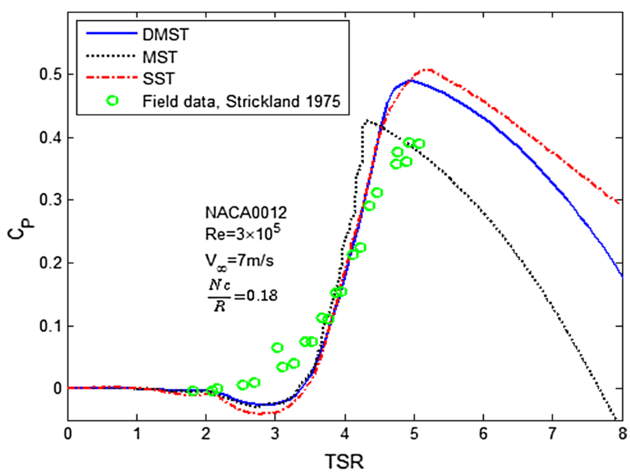

Fig. 13 Comparison of the models using NACA0012

Table 2 Root-mean-squared error (RMSE)

Data Model	Strickland 1975 RMSE	Sandia 5 m RMSE
SST	0.0672	0.1307
MST	0.0582	0.0631
DMST	0.0648	0.0195

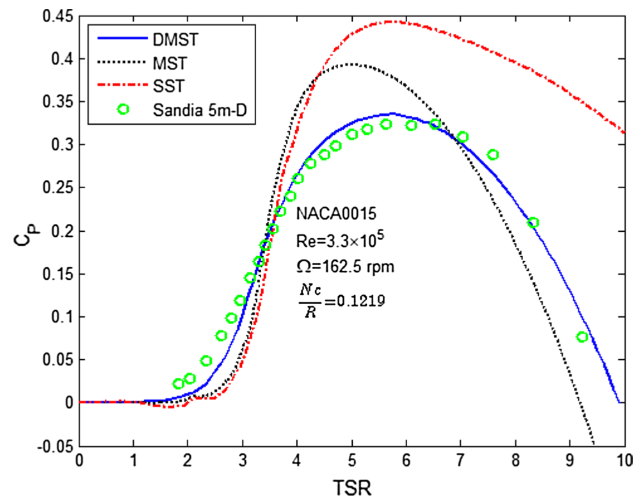

Fig. 14 Comparison of the models using NACA0015

against each other as shown in Fig. 13. As we can see, there is some gap between the experimental data and simulation results which complicates the issue. Thus, the root-mean-squared error (RMSE) is calculated for each model as shown in Table 2. We notice that RMSE values are very close to each other which, again, make it difficult to decide which model is the best; despite, MST model possesses the lowest value of error and seems to be the best model that justifies the need to compare them with other data. To evaluate the models further using a different airfoil, the experimental data for Sandia 5 m turbine (Table 1) were used. The obtained results are provided in Fig. 14 which suggest the superiority of DMST model over SST and MST models, where the latter both overpredict the performance with SST model being the worst. To make it clearer, the RMSE is also calculated as listed in Table 2; we found that DMST model have the lowest error followed by MST and finally SST model. Thus, we concluded that DMST is the best compared to other streamtube models.

4.2 The Effect of Different Airfoils

Using the parameters of Sandia 5-m-diameter VAWT, two more airfoils were considered, namely NACA0012 and NACA0021. The obtained results are reported in Fig. 15. As shown, SST model overestimates the performance in all three cases, and MST model reserves discrepancy in different cases which conclude the goodness of DMST model as it adequately fits the field data. Another version of Fig. 15 is given in Fig. 16 where the performance using specific model is compared by varying the airfoil used, which once again evidences that DMST is superior to SST and MST.

According to Figs. 15 and 16 NACA0015 is the best when compared with NACA0012 and NACA0021 since NACA0015 has better starting torque capacity than NACA0012 and better overall power than NACA0021 (Fig. 17) which make it superior to both.

The maximum power coefficient obtained and the corresponding TSR for each case are summarized in Table 3.

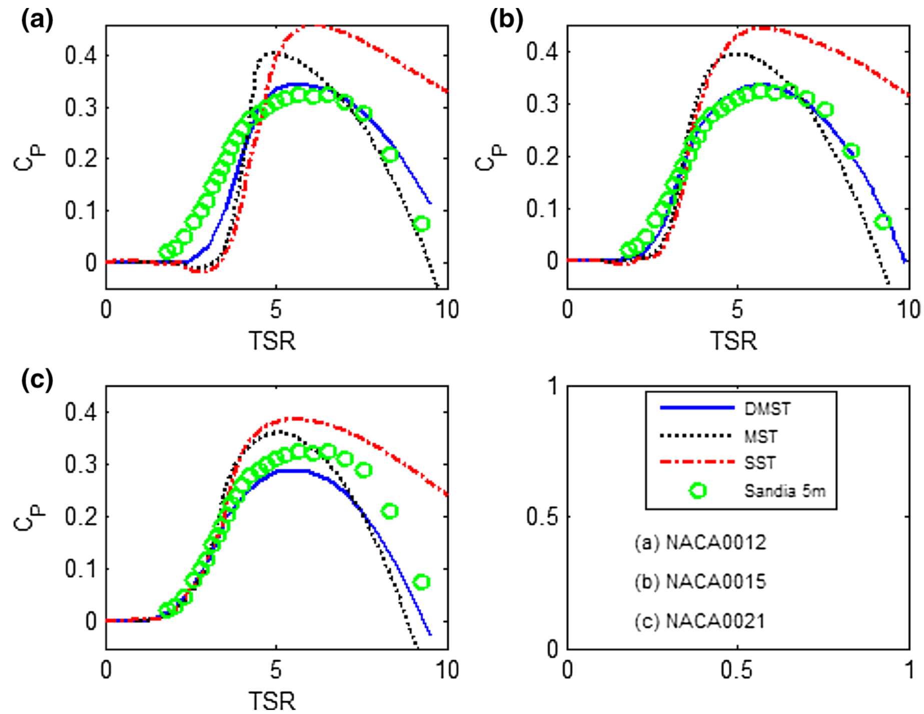

Fig. 15 Comparison of different models using different airfoils

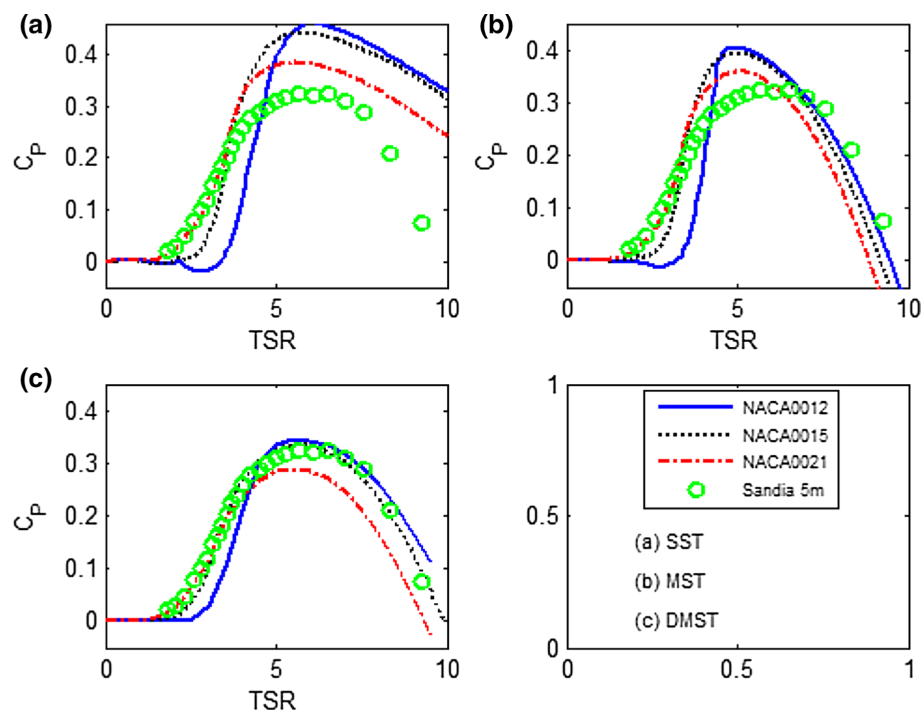

Fig. 16 Comparison of performance under different airfoils using different models

4.3 The Effect of Different Number of Blades

As evidenced from previous results, DMST model has best fitted the experimental data when NACA0015 is utilized Fig. 16. In this section, the results of different models using this profile while changing the number of blades is compared to study their effect on the power coefficient using the parameters of Sandia 5 m turbine. The obtained results are shown in Figs. 18 19 and Table 4. As shown in Fig. 18, the two blades arrangement provides smooth curve over a wide range of TSR with adequate power coefficient which qualify it over 3 and 4 blades. Moreover, increasing the number of blades mean higher rotor solidity which may cause some convergence issues specially for DMST model. As shown in

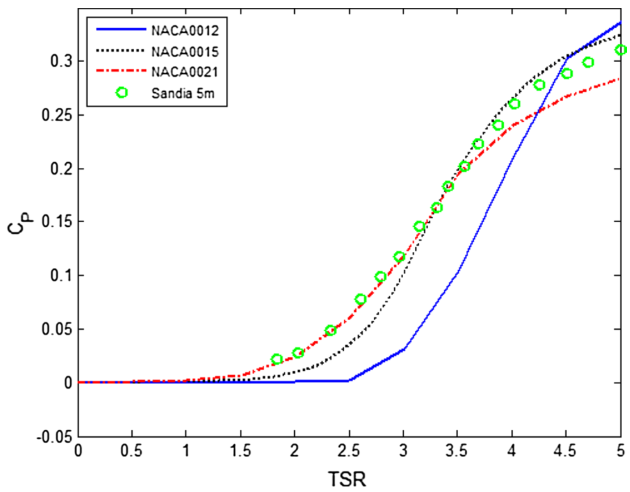

Fig. 17 Comparison of the three airfoils using DMST model

Fig. 19 using DMST is not possible to go beyond a TSR of 6 (8) for 4 (3) blades arrangement which mean the effective TSR zone is very limited, and thus, two-blade configuration is suggested for the small-scale VAWT being investigated.

The performance of Sandi 5 m turbine under different aspect ratios (height/diameter) using DMST model is given in Figs. 20 and 21 by changing the turbine height and diameter, respectively. In Fig. 20, the rotor diameter is kept at 5 m while changing the height. It is found that increasing the aspect ratio from 0.2 to 1.02 greatly increases the peak power coefficient, whereas beyond 1.02 (the design aspect ratio) the improvement rate of peak power significantly decreases which suggests the useless of exceeding the aspect ratio of 2, as there is almost no improvement thereafter. On other hand, the starting capacity declines by increasing the turbine aspect ratio which suggests that an aspect ratio of 1.5 or less is recommended to achieve great peak power with a reasonable starting capacity.

Finally, in Fig. 21, we kept the turbine height at 5.1 m and changed the diameter. We notice that both the peak power and starting capacity are increased by increasing the

Table 3 Maximum power coefficient for different cases

Airfoil	NACA0012		NACA0015		NACA0021	
Model	Max CP	TSR	Max CP	TSR	Max CP	TSR
SST	0.4616	6.000	0.4416	5.7500	0.3841	5.5000
MST	0.4025	4.9500	0.3922	5.0250	0.3587	5.0850
DMST	0.3453	5.5100	0.3346	5.7100	0.2888	5.5100

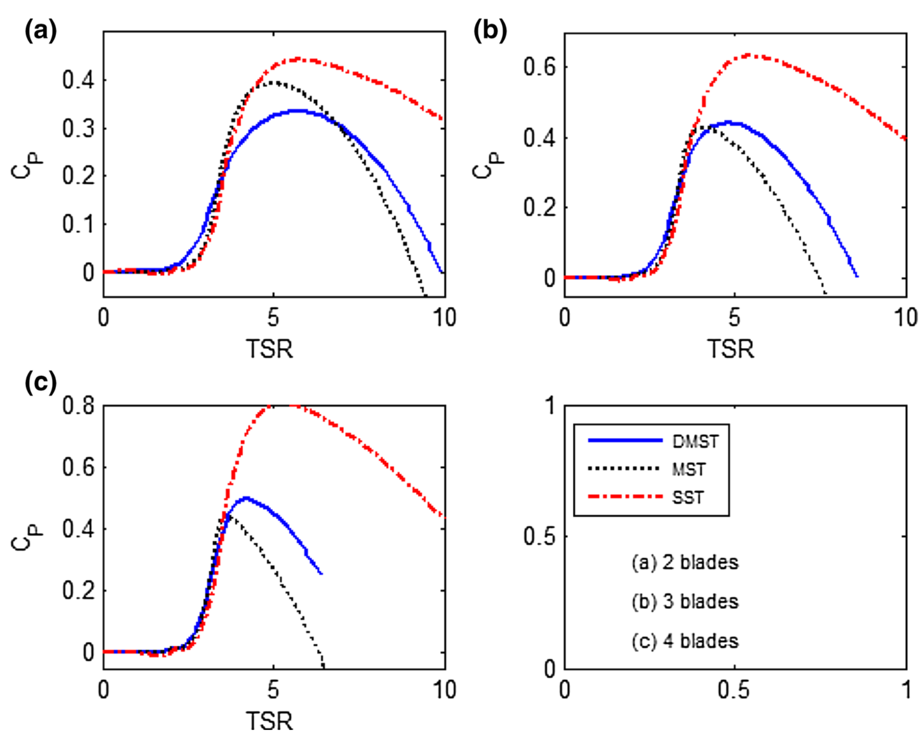

Fig. 18 Comparison of different models using NACA0015 considering different number of blades

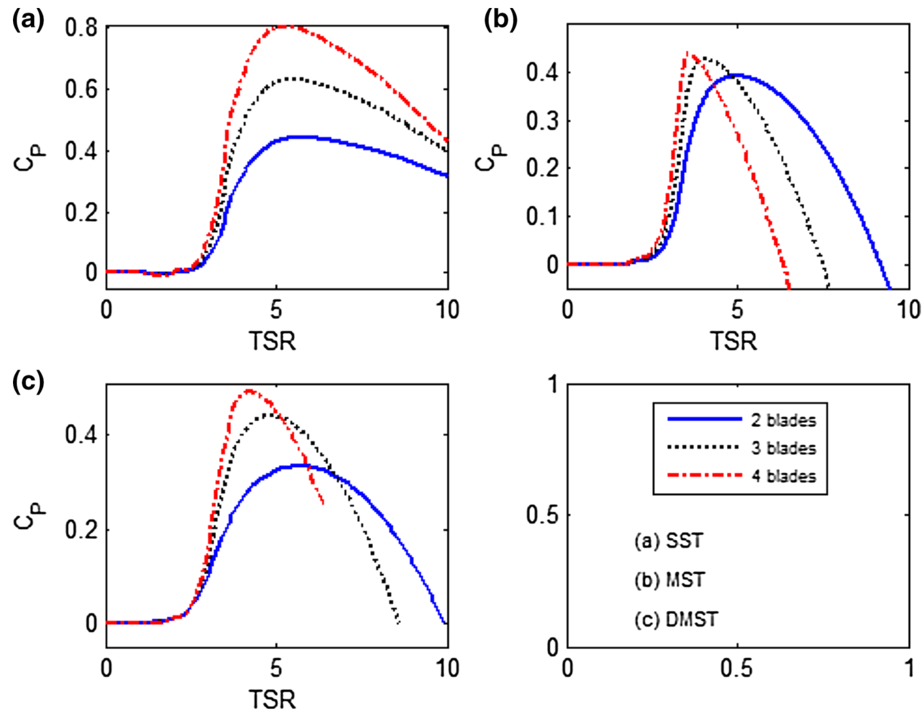

Fig. 19 Comparison of performance under different number of blades using different models with NACA0015

Table 4 Maximum power coefficient considering different number of blades using NACA0015

Blades	2 blades		3 blades		4 blades	
Model	Max CP	TSR	Max CP	TSR	Max CP	TSR
SST	0.4416	5.7500	0.6311	5.4500	0.8041	5.2000
MST	0.3922	5.0250	0.4276	4.0500	0.4415	3.5500
DMST	0.3346	5.7100	0.4408	4.8100	0.4939	4.2100

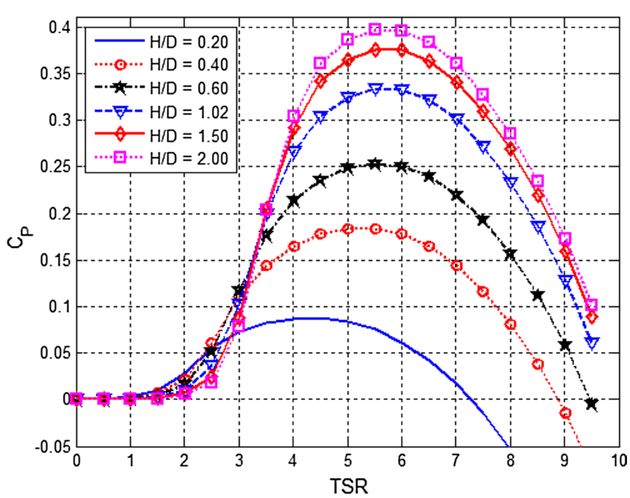

Fig. 20 Power coefficient for Sandia 5 m rotor using DMST model considering different aspect ratios (turbine diameter is kept at 5 m while changing its respective height)

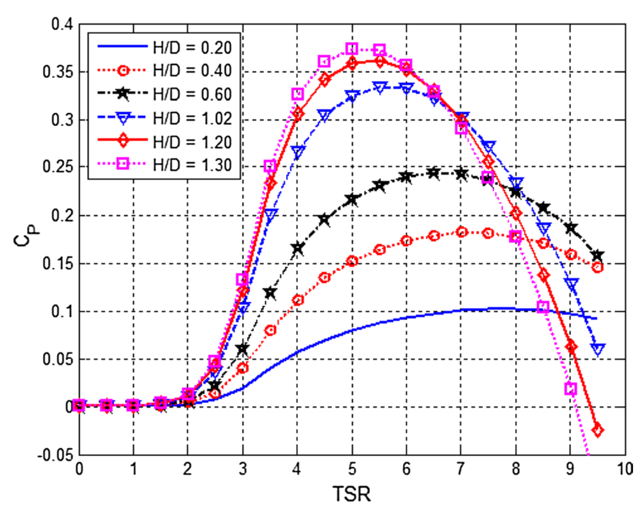

Fig. 21 Power coefficient for Sandia 5 m rotor using DMST model considering different aspect ratios (turbine height is kept at 5.1 m while changing its respective diameter)

aspect ratio (decreasing the rotor diameter); nevertheless, the maximum TSR that could be reached is a bit limited compared with the cases of lower aspect ratios. Therefore, construction and testing of VAWT of 5.1 m height and 4.25 m diameter to achieve a maximum power coefficient of 36.13% at TSR of 5.51 with good starting behavior is recommended.

5 Conclusions

Three streamtube models for VAWTs are compared in this paper. A parametric study is performed, and the obtained results reveal that DMST model is superior over SST & MST models, where the latter two overpredict the performance with SST model being the worst especially at high rotor solidities. Moreover, three different airfoils including NACA0012, NACA0015 and NACA 0021 are considered. It is found that among those profiles, NACA0015 provides reasonable results with maximum power coefficient of around 0.40 for 2-bladed rotor using either SST or MST model and 0.33 when DMST is used. Furthermore, using NACA0015, the effect of turbine solidity is investigated by changing the number of blades for a fixed chord. The superiority of two blades arrangement using NACA0015 is established and acceptable curve pattern for all three models is achieved. We recommend the construction of a testing prototype of two blades rotor with NACA0015 airfoils for good performance characteristics. For different aspect ratios, it is found that the peak power coefficient is directly proportional to the aspect ratio; however, the improvement rate of peak power significantly decreases beyond the design aspect ratio of the turbine which suggests the useless of exceeding twice the design aspect ratio. Finally, a VAWT of 5.1 m height, aspect ratio of 1.2 will achieve a maximum power coefficient of 36.13% at TSR of 5.51 with good starting behavior.

Acknowledgements The authors are grateful for the support of their funding body represented by the Deanship of Scientific Research (DSR) at King Fahd University of Petroleum and Minerals (KFUPM) through the National Science, Technology and Innovation Plan (NSTIP) of the King Abdulaziz City for Science and Technology (KACST): Grant Number 14-ENE2337-04. Moreover, the first author extends his thanks to KFUPM Endowment through Mr. Luhaidan Scholarship Program.

Appendix A

The mathematical relations for momentum models are presented in this section, more details are available in [30].

A.1 General Relations

$$V_c = R\omega + V_a \cos\theta \tag{A.1}$$

$$V_n = V_a \sin\theta \tag{A.2}$$

$$W = \sqrt{V_n^2 + V_c^2} = \sqrt{\left(V_a \sin\theta\right)^2 + \left(R\omega + V_a \cos\theta\right)^2} \tag{A.3}$$

Using free stream velocity, the relative velocity can be expressed in non-dimensional form (a is the axial induction factor and α is the angle of attach:

$$\frac{W}{V_\infty} = \sqrt{((1-a)\sin\theta)^2 + (\lambda + (1-a)\cos\theta)^2} \tag{A.4}$$

$$\alpha = \tan^{-1}\left(\frac{V_n}{V_c}\right) = \tan^{-1}\left[\frac{V_a \sin\theta}{R\omega + V_a\cos\theta}\right] \tag{A.5}$$

Recall that $V_a = V_\infty(1-a)$ and the tip-speed ratio (TSR) $\lambda = R\omega/V_\infty$ previous equation can be written as:

$$\alpha = \tan^{-1}\left[\frac{(1-a)\sin\theta}{\lambda + (1-a)\cos\theta}\right] \tag{A.6}$$

$$C_t = C_l \sin\alpha - C_d \cos\alpha \tag{A.7}$$

$$C_n = C_l \cos\alpha + C_d \sin\alpha \tag{A.8}$$

where C_l and C_d are the airfoil lift and drag coefficients, respectively, and C_n is the normal coefficient.

$$F_t = \frac{1}{2}C_t\rho cHW^2 \quad \text{and} \quad F_n = \frac{1}{2}C_n\rho cHW^2 \tag{A.9}$$

F_t and F_n are the tangential and normal forces, respectively. Different models were developed to calculate such forces.

$$F_{ta} = \frac{1}{2\pi}\int_0^{2\pi} F_t(\theta)\mathrm{d}\theta \tag{A.10}$$

The total torque (Q) for the number of blades (N) is found as

$$Q = NF_{ta}R \tag{A.11}$$

The total power (P) can be obtained as

$$P = Q \times \omega \tag{A.12}$$

A.2 Single Streamtube Model

Owing to the rate of change of momentum, the streamwise drag force (F_D) is given by [19]:

$$F_D = 2\rho AV_a(V_\infty - V_a) \tag{A.13}$$

The rotor drag coefficient (C_{DD}) is defined as

$$C_{DD} = \frac{F_D}{\frac{1}{2}\rho AV_a^2} = \frac{4(V_\infty - V_a)}{V_a} \tag{A.14}$$

$$\frac{V_a}{V_\infty} = \left(\frac{1}{1 + C_{DD}/4}\right) \tag{A.15}$$

$$C_{\mathrm{D}}=\frac{F_{\mathrm{D}}}{\frac{1}{2}\rho AV_{\infty}^{2}}=C_{\mathrm{DD}}\left(\frac{V_{\mathrm{D}}}{V_{\infty}}\right)=\frac{C_{\mathrm{DD}}}{\left(1+\frac{1}{4}C_{\mathrm{DD}}\right)^{2}} \tag{A.16}$$

The local relative dynamic pressure is given by:

$$\frac{q}{\frac{1}{2}\rho AV_{a}^{2}}=\left(\frac{R\omega}{V_{a}}+\cos\theta\right)^{2}+\sin^{2}\theta=\left(\frac{W}{V_{a}}\right)^{2} \tag{A.17}$$

The total drag of a rotor having N blades read as:

$$F_{\mathrm{D}}=\frac{NcH}{2\pi}\int_{0}^{2\pi}q\left(C_{\mathrm{n}}\sin\theta-C_{\mathrm{t}}\cos\theta\right)\mathrm{d}\theta \tag{A.18}$$

Thus, considering a straight-bladed rotor of height H and radius R, the area $A=2HR$

$$C_{\mathrm{D}}=\frac{Nc}{R}\frac{1}{2\pi\rho V_{a}^{2}}\int_{0}^{2\pi}q\left(C_{\mathrm{n}}\sin\theta-C_{\mathrm{t}}\cos\theta\right)\mathrm{d}\theta \tag{A.19}$$

The tip-speed ratio, (TSR) is calculated as:

$$\lambda=\frac{R\omega}{V_{\infty}}=\frac{R\omega}{V_{a}}\left(\frac{1}{1+\frac{1}{4}C_{\mathrm{DD}}}\right) \tag{A.20}$$

The total torque of the rotor is given by:

$$T=\frac{NcRH}{2\pi}\int_{0}^{2\pi}qC_{\mathrm{t}}\mathrm{d}\theta \tag{A.21}$$

The power is given by:

$$P=\omega\times T=\frac{NcRH\omega}{2\pi}\int_{0}^{2\pi}qC_{\mathrm{t}}\mathrm{d}\theta \tag{A.22}$$

The maximum possible power, according to the Betz limit, is given by Paraschivoiu [19] and Mohammed et al. [30]:

$$P_{\max}=\frac{32}{27}\frac{1}{2}\rho V_{\infty}^{3}RH \tag{A.23}$$

The power coefficient is thus:

$$C_{\mathrm{P}}=\frac{P}{P_{\max}}=\frac{27}{32}\frac{1}{2\pi}\frac{Nc}{R}\frac{R\omega}{V_{a}}\left(\frac{V_{a}}{V_{\infty}}\right)^{3}\int_{0}^{2\pi}\left(\frac{q}{\frac{1}{2}\rho V_{a}^{2}}\right)C_{\mathrm{t}}\mathrm{d}\theta \tag{A.24}$$

A.3 Multiple Streamtube Model

The average streamwise force $\overline{F_x}$ applied by blade elements while passing the streamtube is found from [19]:

$$\overline{F_{x}}=2\rho AV_{a}\left(V_{\infty}-V_{a}\right)=NF_{x}\frac{\Delta\theta}{\pi} \tag{A.25}$$

$$\frac{NF_{x}}{2\pi\rho r\Delta h\sin\theta V_{\infty}^{2}}=\frac{V_{a}}{V_{\infty}}\left(1-\frac{V_{a}}{V_{\infty}}\right)=F_{x}^{*} \tag{A.26}$$

$$F_{x}=-\left(F_{\mathrm{N}}\sin\theta+F_{\mathrm{T}}\cos\theta\right) \tag{A.27}$$

$$F_{x}^{*}=\frac{NF_{x}}{2\pi\rho r\Delta h\sin\theta V_{\infty}^{2}}=\frac{NC}{4\pi r}\left(\frac{W}{V_{\infty}}\right)^{2}\left(C_{\mathrm{n}}-C_{\mathrm{t}}\frac{\cos\theta}{\sin\theta}\right) \tag{A.28}$$

$$a=1-\frac{V_{a}}{V_{\infty}} \tag{A.29}$$

$$a=F_{x}^{*}+a^{2} \tag{A.30}$$

This is a fundamental relation to solve the streamtube momentum equation iteratively.

The torque produced by a single blade is given by:

$$T_{\mathrm{B}}=\frac{1}{2}\rho cHW^{2}C_{\mathrm{t}}R \tag{A.31}$$

The average total torque produced by the rotor is written as:

$$T=\frac{N}{N_{\theta}}\sum_{1}^{N_{\theta}}T_{\mathrm{B}} \tag{A.32}$$

where $N_{\theta}=\frac{\pi}{\Delta\theta}+1$ and $\Delta\theta$ is the size of streamtube.

The power coefficient is given as follows:

$$C_{\mathrm{P}}=\frac{T\omega}{\frac{1}{2}\rho AV_{\infty}^{2}}=\frac{\sum_{1}^{N_{\theta}}\frac{NC}{2R}\lambda\left(\frac{W}{V_{\infty}}\right)^{2}C_{\mathrm{t}}}{N_{\theta}} \tag{A.33}$$

A.4 Double Multiple Streamtube Model

As mentioned before, the calculation are performed twice for upwind half ($\pi/2\le\theta\le3\pi/2$) and for downwind half ($3\pi/2\le\theta\le\pi/2$) cycles. Equations (A.3) and (A.6) are used to find the relative velocity and angle of attach, respectively. Equating the forces given by momentum equations to those given by blade element theory [19, 31]:

$$f_{\mathrm{u}}(1-a)=a \tag{A.34}$$

where the upwind function f_u is given by:

$$f_{\mathrm{u}} = \frac{Nc}{8\pi R} \int_{\pi/2}^{3\pi/2} \left(C_{\mathrm{n}} \frac{\cos\theta}{|\cos\theta|} - C_{\mathrm{t}} \frac{\sin\theta}{|\sin\theta|} \right) \left(\frac{W}{V_a} \right)^2 \mathrm{d}\theta \quad (A.35)$$

Thus, the power coefficient for the upwind half of the turbine is given by:

$$C_{\mathrm{P}_u} = \frac{NcH}{2\pi A} \int_{\pi/2}^{3\pi/2} C_{\mathrm{t}} \left(\frac{W}{V_\infty} \right)^2 \mathrm{d}\theta \quad (A.36)$$

The downwind part of the rotor is treated similarly and finally the power coefficients of the two half cycles is summed to find the overall power coefficient of the rotor.

References

1. Ackermann, T.; Söder, L.: Wind energy technology and current status: a review. Renew. Sustain. Energy Rev. **4**(4), 315–374 (2000)
2. Thresher, R.W.; Robinson, M.C.; Veers, P.S.: Wind Energy Technology: Current Status and R&D Future. National Renewable Energy Laboratory, Golden (2008)
3. Al-Douri, Y.; Waheeb, S.; Voon, C.: Review of the renewable energy outlook in Saudi Arabia. J. Renew. Sustain. Energy **11**(1), 015906 (2019)
4. Eltamaly, A.M.; Addoweesh, K.E.; Bawa, U.; Mohamed, M.A.: Economic modeling of hybrid renewable energy system: a case study in Saudi Arabia. Arab. J. Sci. Eng. **39**(5), 3827–3839 (2014)
5. Eltamaly, A.M.: Pairing between sites and wind turbines for Saudi Arabia Sites. Arab. J. Sci. Eng. **39**(8), 6225–6233 (2014)
6. Herbert, G.J.; Iniyan, S.; Sreevalsan, E.; Rajapandian, S.: A review of wind energy technologies. Renew. Sustain. Energy Rev. **11**(6), 1117–1145 (2007)
7. Cooper, P.: Development and analysis of vertical-axis wind turbines. In: Tong, W. (ed.) WIT Transactions on State of the Art in Science and Engineering, vol. 1, 1st edn, pp. 277–302. WIT Press, Southampton (2010)
8. Schaffarczyk, A.P.: Types of wind turbines. In: Schafarczyk, A.P. (ed.) Introduction to Wind Turbine Aerodynamics, pp. 7–20. Springer, Berlin (2014)
9. Jin, X.; Zhao, G.; Gao, K.; Ju, W.: Darrieus vertical axis wind turbine: basic research methods. Renew. Sustain. Energy Rev. **42**, 212–225 (2015)
10. Brusca, S.; Lanzafame, R.; Messina, M.: Design of a vertical-axis wind turbine: how the aspect ratio affects the turbine's performance. Int. J. Energy Environ. Eng. **5**(4), 333–340 (2014)
11. Rezaeiha, A.; Montazeri, H.; Blocken, B.: Effect of solidity on aerodynamic performance of vertical axis wind turbines. In: XV Conference of the Italian Association for Wind Engineering (IN-VENTO 2018), 9–12 September 2018, Napoli, Italy (2018)
12. Kanyako, F.; Janajreh, I.: Vertical axis wind turbine performance prediction models using high and low fidelity analyses. Int. J. Eng. Res. Innov. **7**, 48–56 (2015)
13. Beri, H.; Yao, Y.; et al.: Double multiple streamtube model and numerical analysis of vertical axis wind turbine. Energy Power Eng. **3**(03), 262 (2011)
14. Zhu, H.; Li, C.; Hao, W.; Ding, Q.; Yu, W.: Investigation on aerodynamic characteristics of building augmented vertical axis wind turbine. J. Renew. Sustain. Energy **10**(5), 053302 (2018)
15. Peng, H.; Lam, H.; Liu, H.: Numerical investigation into the blade and wake aerodynamics of an H-rotor vertical axis wind turbine. J. Renew. Sustain. Energy **10**(5), 053305 (2018)
16. Saeidi, D.; Sedaghat, A.; Alamdari, P.; Alemrajabi, A.A.: Aerodynamic design and economical evaluation of site specific small vertical axis wind turbines. Appl. Energy **101**, 765–775 (2013)
17. Bouzaher, M.T.; Hadid, M.: Numerical investigation of a vertical axis tidal turbine with deforming blades. Arab. J. Sci. Eng. **42**(5), 2167–2178 (2017)
18. Wang, T.: A brief review on wind turbine aerodynamics. Theor. Appl. Mech. Lett. **2**(6), 062001-1–062001-18 (2012)
19. Paraschivoiu, I.: Wind Turbine Design: With Emphasis on Darrieus Concept. Presses inter Polytechnique, Montreal (2002)
20. Templin, R.: Aerodynamic Performance Theory for the NRC Vertical-Axis Wind Turbine. National Aeronautical Establishment, Ottawa (1974)
21. Strickland, J.H.: Darrieus Turbine: A Performance Prediction Model Using Multiple Streamtubes. Sandia Labs., Albuquerque (1975)
22. Sanyer, W.: The development of a wind turbine for residential use. Master thesis, North Carolina State University, Raleigh, NC (2011)
23. Batista, N.; Melício, R.; Mendes, V.M.; Figueiredo, J.; Reis, A.: Darrieus wind turbine performance prediction: computational modeling. In: Doctoral Conference on Computing, Electrical and Industrial Systems, pp. 382–391 (2013)
24. Paraschivoiu, I.: Double-multiple streamtube model for Darrieus in turbines. In: Wind Turbine Dynamics, Second DOE/NASA Wind Turbines Dynamics Workshop, Cleveland, OH (1981)
25. Yang, Y.; Guo, Z.; Zhang, Y.; Jinyama, H.; Li, Q.: Numerical investigation of the tip vortex of a straight-bladed vertical axis wind turbine with double-blades. Energies **10**(11), 1721-1–1721-18 (2017)
26. Ferrari, G.: Development of an aeroelastic simulation for the analysis of vertical-axis wind turbines. ResearchSpace@ Auckland (2012)
27. Zhao, Z.; et al.: Study on variable pitch strategy in H-type wind turbine considering effect of small angle of attack. J. Renew. Sustain. Energy **9**(5), 053302 (2017)
28. Sheldahl, R.E.: Aerodynamic characteristics of seven airfoil sections through 180 degrees angle of attack for use in aerodynamic analysis of vertical axis wind turbines. SAND80-2114 (1981)
29. Sheldahl, R.E.; Klimas, P.C.; Feltz, L.V.: Aerodynamic performance of a 5-metre-diameter Darrieus turbine with extruded aluminum NACA-0015 blades. NASA STI/Recon technical report N, vol. 80 (1980)
30. Mohammed, A.A.; Ouakad, H.M.; Sahin, A.Z.; Bahaidarah, H.M.: Vertical axis wind turbine aerodynamics: summary and review of momentum models. J. Energy Res. Technol. **141**(5), 050801 (2019)
31. Goude, A.: Fluid mechanics of vertical axis turbines simulations and model development. Acta Universitatis Upsaliensis, Uppsala (2012)